

HYDRODYNAMIC MODELLING OF EXTREME FLOOD LEVELS IN AN ESTUARY DUE TO CLIMATE CHANGE

JK Vonkeman, PhD Student, Department of Civil Engineering, University of Stellenbosch, Stellenbosch, South Africa

O Sawadogo, Hydraulic Modeler & Researcher, Department of Civil Engineering, University of Stellenbosch, Stellenbosch, South Africa

DE Bosman, Senior Coastal Engineer, Department of Civil Engineering, University of Stellenbosch, Stellenbosch, South Africa

GR Basson, Professor, Head: Water Division, Department of Civil Engineering, University of Stellenbosch, Stellenbosch, South Africa, grbasson@sun.ac.za

Abstract

The determination of extreme flood levels in an estuary should consider river floods and waves penetrating the estuary. The Breede River estuary in South Africa, 50 km in length, is discussed as case study in this paper. A two-dimensional hydrodynamic model Mike21C of the DHI Group of the 50km estuary (including the estuary mouth) was set up and calibrated against historical flood levels (1906 and 2008), and field data (tidal level, flow velocities and sediment transport) obtained during 2017. The model was then used to route the 100-year flood with a peak of 3789 m³/s through the entire estuary. The flood included an increase of 15% for future climate change. Open and initially closed estuary mouth conditions were investigated with the movable bed model. For future climate change scenarios the initial closed estuary mouth berm crest level was selected as 3.5 masl and the hydrodynamic model simulated the breaching of the berm as the flood hydrograph was routed through the estuary. Based on the 2013 AR5 report of the IPCC sea level rise predictions due to climate change, sea level rise values of 0.5 m and 1.0 m in 50 and 100 years' time respectively, were assumed for the study. The initial estuary bed levels were also raised correspondingly along the full length of the estuary for the future scenarios due to expected sediment deposition.

The tidal boundary in the hydrodynamic model was set constant at the respective recurrence interval maximum tidal levels (based on observed data) and a long wave with a height of 0.7 m and a period of 180 s was also specified at the open boundary to include the effect of infragravity waves associated with wave grouping of shorter period stormy waves. (The penetration of the shorter period stormy waves into the estuary and associated wave runup were treated separately). From the output of the MIKE21C model the maximum simulated water levels in the model domain were obtained, and the velocity heads were added, to obtain the energy levels which account for turbulent flow wave action. In order to determine the floodline levels for the Breede River Estuary, the runup of the shorter period stormy waves on the estuary banks were also obtained by modelling the penetration of the shorter period stormy waves with SWAN and the consequent wave runup was then determined with empirical methods. The final floodline levels were determined by adding the wave runup heights of the shorter period stormy waves to the maximum routed flood levels.

Short period waves originating from deep sea (swell) in combination with locally generated wind waves can penetrate an open estuary mouth and therefore can contribute to more extensive flood

levels when its consequent wave runup is superimposed on a concurrent river flood level. For this purpose, waves from the most critical direction causing maximum penetration into the lower estuary (i.e. waves from the east-southeasterly direction) were transferred from deep sea through an open mouth into the estuary by means of the nearshore wave model, SWAN. The transfer of the east-southeasterly swell from deep sea was done concurrently with a local wind blowing from the same sector over the entire SWAN model area. The resultant wave penetration into the estuary was therefore a combination of deep sea swell and locally wind generated waves. The 100-year wave and wind conditions were used to determine the spatial distribution of the penetrated wave conditions in the estuary and its consequent wave runup at eight locations in the lower estuary. The highest flood line level (flood energy level plus wave runup height) of 8.1 masl was calculated near the mouth for the future climate change scenario, 100 years from the present.

Keywords

Extreme flood, climate change, flood routing; estuary, wave penetration; wave runup

Introduction

The determination of extreme flood levels in an estuary should consider river floods and waves penetrating the estuary. Floodlines were determined for the Breede River estuary in the Western Cape, South Africa, from about 10 km upstream of Malgas to the mouth at Witsand, which is discussed as a case study in this paper (Figure 1). The scope of work includes flood hydrology determination, field work for hydrodynamic model setup and calibration, hydrodynamic modelling of flood levels caused by extreme floods, but also considering wave penetration through an open mouth during storms. Climate change was accounted for in future scenarios by modelling the sea level raised by 0.5 m and 1.0 m in 50 and 100 years' time respectively.



Figure 1. Location of the study area in Africa

Field Measurements

Three different aspects of field work were done for the setup and calibration of the hydrodynamic modelling:

1. Local residents and representatives of the Malgas and Witsand communities identified reliable historical flood markers along the Breede River Estuary which were surveyed by a Trimble GPS. A total of nine markers were measured for the 2008 flood with one

additional marker for the 1906 flood at the Malagas Church. The surveyed flood levels were also checked against the LiDAR survey data. The aerial photograph in Figure 2, provided by Mr Peter Müller illustrates the extent of the 2008 flood in the Breede River Estuary.

2. An underwater bathymetric survey of the 50km extent of the Breede River Estuary was done because no sufficiently reliable historical underwater survey data was available. The bathymetric survey was carried out from a small boat with Sontek Rivercat Acoustic Doppler Current Profiler (ADCP) equipment followed by post-processing on HYPACK software.
3. Sediment transport near the mouth of the river (bedload and suspended sediment sampling), was carried out using standard USGS equipment. Flow velocity and discharge was also measured at these five sites by the ADCP, while a Department of Water and Sanitation (DWS) pressure gauge and logger was used to record the water levels in the estuary. Finally, 25 bed sediment grab samples were collected along the full length of the estuary for grading analysis. The average median sediment size was found to be 0.35 mm, while near the mouth the marine sediment has an average median size of about 0.50 mm.



Figure 2. Aerial photograph of 2008 flood along the Breede River Estuary

Flood Hydrology and Risk

The probability of a flood peak that has a 1% chance of being exceeded in any year is described as a 100-year flood event. However, the Annual Exceedance Probability (AEP) avoids the common misconception that, for example, a 100-year flood can only occur once every 100 years. The actual risk of experiencing different flood events is summarized in Table 1. A conservative approach in the study has been assumed whereby the same recurrence interval for the flood, wave, wind and tidal level occurred simultaneously. This is not an unrealistic approach since the values for the recurrence intervals do not differ significantly. However, the joint probability of an extreme flood occurring simultaneously with an extreme wind velocity will of course be less than the selected individual probabilities of a flood and a wind velocity.

The flood hydrology was calculated by using probabilistic methods (average of the Log-Normal and Log-Pearson Type 3) of observed historical flood records. The annual recurrence interval floods used in this study for the future 50- and 100-year floods are 3196 and 3789 m³/s at the mouth, and include 15% increase for future climate change impacts and 10% for flow measurement inaccuracy. For the current scenario these floods are 2779 and 3295 m³/s, for the 50- and 100-year floods respectively.

Table 1. Probabilities of experiencing a given size flood once or more in a lifetime

| Size of flood (chance of occurrence in any year) ARI/AEP | Probability of experiencing the given flood in a period of 70 years | |
|---|---|--------------------|
| | At least once (%) | At least twice (%) |
| 1 in 10 (10 %) | 99.9 | 99.3 |
| 1 in 20 (5 %) | 97.0 | 86.4 |
| 1 in 50 (2 %) | 75.3 | 40.8 |
| 1 in 100 (1 %) | 50.3 | 15.6 |
| 1 in 200 (0.5 %) | 29.5 | 4.9 |

Based on field work and hydrodynamic modelling, the 1906 flood was calibrated against the flood mark at the Malagas Church and found to be 2700 m³/s. Compared to the historical flood peak data, this 1906 corresponds to about a historical 1:80 year flood event. The 2008 flood peak is estimated to be 1546 m³/s, based on the extrapolated DWS gauging station stage-discharge rating, and has an annual recurrence interval of minimum 25 years based on the historical data.

The Effect of Climate Change

Sea level rise

The International Panel for Climate Change (IPCC) has issued five Assessment Reports (AR) since its establishment in 1988. The projected sea level rise for the South African south coast presented in Table 2 was based on the Fifth Assessment Report (AR5) of the IPCC in 2013/14. The sea level rise projections of the IPCC are based on the 5 – 95% projection ranges of 21 CMIP5 (Coupled Model Intercomparison Project Phase 5) climate models for the 2046-2065 and 2081–2100 periods under different RCP (Representative Concentration Pathway) scenarios. It is recommended that the maximum rise in sea level due to climate change should be taken as 0.5 m and 1.0 m in 50 and 100 years' time respectively.

Table 2. Estimation of projections of sea level rise for the South African south coast

| Scenario | 2046 - 2065 | | | | 2081 - 2100 | | | |
|----------|-------------|--------------|----|-------------|-------------|--------------|----|-------------|
| | Mean | Likely range | | | Mean | Likely range | | |
| RCP2.6 | 0.28 | 0.20 | to | 0.37 | 0.46 | 0.30 | to | 0.64 |
| RCP4.5 | 0.30 | 0.22 | to | 0.38 | 0.54 | 0.37 | to | 0.73 |
| RCP6.0 | 0.29 | 0.21 | to | 0.37 | 0.56 | 0.38 | to | 0.73 |
| RCP8.5 | 0.35 | 0.25 | to | 0.44 | 0.73 | 0.52 | to | 0.95 |

Change in wind conditions due to climate change

According to the information on projected change in wind velocity due to climate change from the IPCC AR5, it is evident that the projected change in wind velocity (both for the daily averaged and 99th percentile of the daily averaged velocities) is very small on the SA south coast. However, the projected change in wind velocity in the southern ocean close to the polar zone shows an increase of about 10% for daily averaged and 5% for the 99th percentile of the daily

averaged velocities – this is probably due to the shifting of the pathways of the southern extra-tropical cyclones further south to the polar area and probable increase in wind velocity there. Based on the above information, the projected local wind velocities for the Breede River Estuary study was assumed, for the purpose of this study, not to be affected.

Change in wave conditions due to climate change

The projected change in wave conditions due to climate change in the IPCC AR5 (Figure 13.26) indicates a very small change in the projected annual mean significant wave height (SWH) on the SA south coast – an increase of about 1%. The change in projected mean wave period is very small on the SA south coast and the change in projected wave direction is more from the south (a change of about 5° anticlockwise). Subsequent to the publishing of IPCC AR5 (2013), Wang et al. (2014) of the Climate Research Division, Science and Technology, Environment Canada, published work on projected wave height change due to climate change. This study made statistical projections of changes in ocean wave heights using sea level pressure information from 20 CMIP5 (Coupled Model Inter-comparison Project Phase 5) global climate models for the 21st century. From the information in Wang et al. (2014) it can be concluded that although the 1:10 year significant wave height is projected to increase over large portions of the globe (including the southern ocean area close to Antarctica), the projected change close to the SA south coast is very small. From the information in Mentaschi et al. (2017), [which agrees with the predictions of Wang et al. (2014)], it can be stated that the projected 1:100 year wave energy flux shows for the SA south coast a slight increase for 2050 (in the order of 2-3%) and no change for 2100. Based on the above research on projected change in wave height conditions for the period 2070 to 2099, it was assumed for the purpose of this study that the wave conditions are not altered by climate change.

Hydrodynamic Modelling of Floods

Model setup

The 2D fully hydrodynamic model Mike 21C of DHI was used to simulate the flood levels in the Breede River Estuary. In addition, the sediment transport, erosion and deposition were modelled by a movable bed. The model bathymetry was set up by using the LiDAR data as well as the underwater survey as shown in Figure 3. The bathymetry includes the river reach extending 3km upstream of Malgas to 3km into the sea, a total length of approximately 47km. Sea bed levels were obtained from the General Bathymetric Chart of the Oceans (GEBCO). The model used a curvilinear grid 15m wide by 30m long in the flow direction and simulation time steps in the order of 1 second. The runtime for each simulation was approximately 26 hours.

Model calibration against field data

Based on the bed sediment grab samples and spring tide measurements, the hydrodynamic model was calibrated with a Manning n-value of 0.045 as representative bed roughness in the main channel. A bed roughness of 0.060 was selected for the floodplains based on the vegetation heights from the LiDAR ground and non-ground level data, which was also calibrated against the 2008 flood levels.

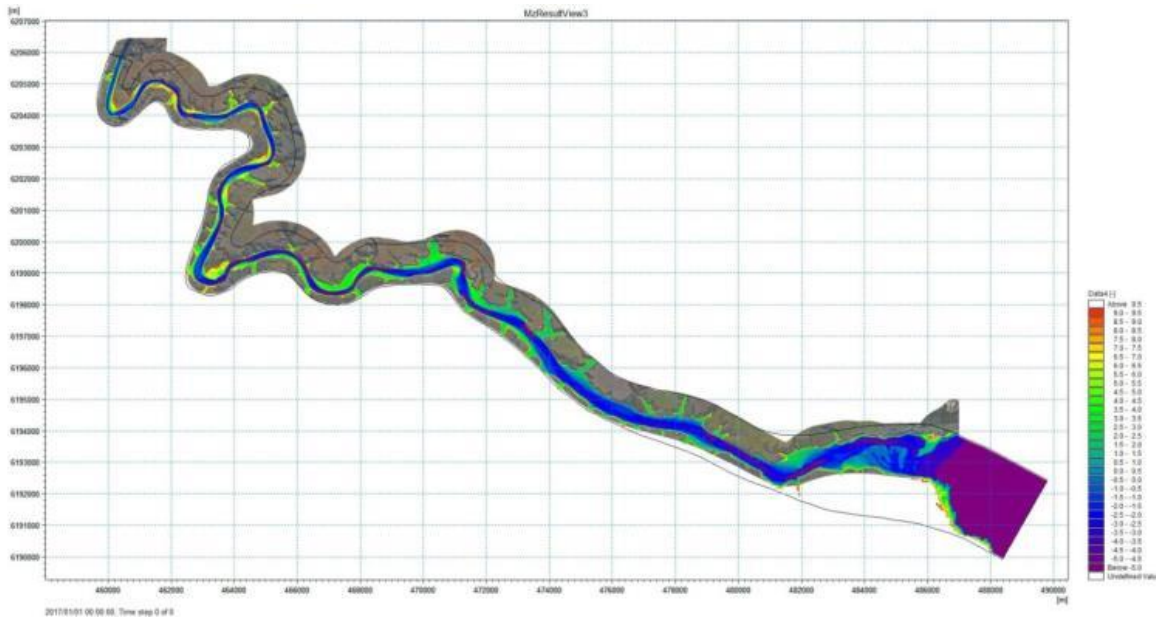


Figure 3. Bathymetry of the Breede River Estuary (masl)

Figure 4 shows the simulated versus observed tidal water levels in the estuary at Witsand tide gauge of DWS (H7T014). Table 3 shows the simulated bed sediment loads, flow velocities and flow depths at the flow measurement transect in the Lower Breede River Estuary, which compare reasonably well with the observed values when one compares the average values of flow depth and of bed load. The simulated flood levels in the Upper Breede River Estuary were also compared with the surveyed flood marks near Malgas for the 2008 flood as indicated in Table 4. On average the simulated flood levels are 0.26 m higher than the observed water levels and are considered acceptable. The 1906 flood was also simulated whereby an inflow discharge of 2 700 m³/s replicated the observed flood level at the Malgas church (Table 5) which could be used in the probabilistic flood analysis. There is of course some uncertainty with the 1906 simulated flood peak due to the assumption that the estuary bed was similar as in the more recent survey.

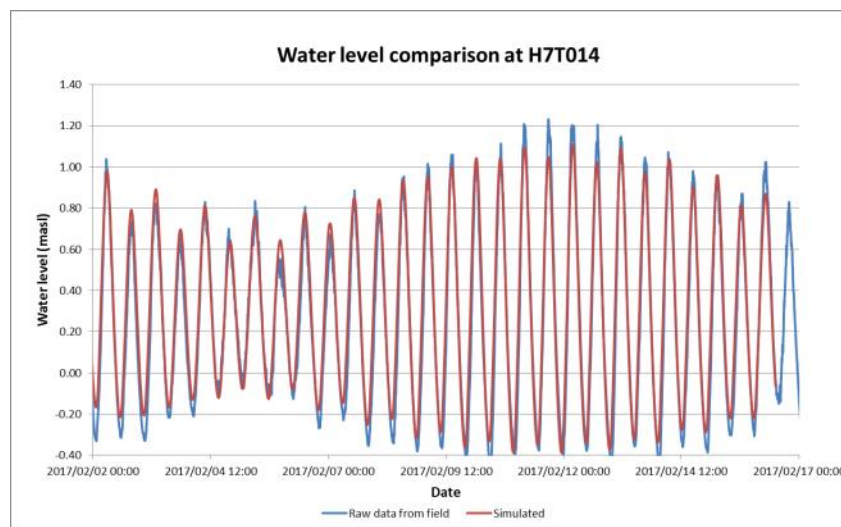


Figure 4. Calibrated water levels in the Breede River Estuary at the DWS tidal gauge H7T014

Table 3. Calibrated flow velocities, depth and bedload in the Lower Breede River Estuary

| Sample sites | Flow velocity (m/s) | | Flow depth (m) | | Bed load (kg/s.m) | |
|----------------|---------------------|-------------|----------------|-------------|-------------------|---------------|
| | Observed | Simulated | Observed | Simulated | Observed | Simulated |
| 20;21 | 0.73 | 0.49 | 5.20 | 5.74 | 0.0065 | 0.0070 |
| 22 | 0.75 | 0.51 | 6.40 | 5.82 | 0.0016 | 0.0102 |
| 23,24 | 0.76 | 0.44 | 5.55 | 4.37 | 0.0170 | 0.0087 |
| Average | 0.75 | 0.48 | 5.72 | 5.31 | 0.0084 | 0.0086 |

Table 4. Simulated 2008 flood levels compared with the surveyed flood marks

| GPS Waypoint | Description | Latitude | Longitude | Observed maximum water level (masl) | Simulated maximum water level (masl) |
|--------------|-------------------|---------------|---------------|-------------------------------------|--------------------------------------|
| 27 | De Kock Patio | 34°17'50.19"S | 20°34'39.32"E | 7.56 | 8.13 |
| 28 | Malagas Church | 34°17'47.61"S | 20°35'03.65"E | 8.37 | 7.86 |
| 29 | Malagas Hotel | 34°18'01.69"S | 20°35'16.79"E | 7.96 | 7.71 |
| 30 | Lemoentuin Steps | 34°19'07.98"S | 20°36'42.64"E | 6.61 | 6.86 |
| 31 | Rob's House | 34°20'27.98"S | 20°35'54.94"E | 5.97 | 6.15 |
| 32 | Diepkloof Gardens | 34°21'12.16"S | 20°36'03.90"E | 5.17 | 6.04 |
| 33 | Riverine Marker | 34°20'49.75"S | 20°36'53.11"E | 5.01 | 5.76 |

Table 5. Simulated 1906 flood level compared with the surveyed flood mark

| GPS Waypoint | Latitude | Longitude | Observed maximum water level (masl) | Simulated maximum water level (masl) | Simulated flood peak (m ³ /s) |
|--------------|---------------|---------------|-------------------------------------|--------------------------------------|--|
| 28 | 34°17'47.61"S | 20°35'03.65"E | 10.05 | 10.15 | 2700 |

Model boundary conditions and scenarios

A total of 18 simulation scenarios with different flood peaks and berm heights were considered as indicated in Figure 5. Climate change was accounted for in future scenarios by modelling the sea level raised by 0.5 m and 1.0 m in 50 and 100 years' time respectively. At the upstream end of the estuary, a 17 day flood hydrograph (with a shape based on the 2008 observed flood) was specified at the model boundary. While at the downstream boundary in the ocean, a constant tidal level was specified as well as a long wave with a height of 0.7 m and a period of 180 s. Maximum tidal levels of 2.07 masl and 2.16 masl were obtained for the 50-year and 100-year return intervals respectively (based on recorded tidal data at Mossel Bay from UHSLC).

Open and closed initial condition estuary mouths were simulated. While the mouth has never closed in the past, it is possible that future land use changes with climate change in the catchment could decrease the drought flow of the Breede River to such an extent and duration, that the mouth could close. The LiDAR survey indicates that the wave over wash builds the beach berm up to 2.5 masl and this is probably realistic for the current scenario. As a sensitivity test a berm crest level of 3.5 masl was, however, also simulated. The hydrodynamic model routes the flood hydrograph through the estuary, fills the lower estuary upstream of a closed initial berm, and eventually spills over the berm, eroding the sandy berm until the berm ultimately breaches. The lowest elevation of the berm crest of the closed initial mouth determines where the mouth will breach first. These lowest levels on the berm are determined by wave over wash events. For future climate change scenarios the initial closed berm crest levels will be higher. It is assumed that the sea level will rise by 0.5 m and 1.0 m in 50 and 100 years' time respectively, due to climate change. The initial estuary bed levels were also raised correspondingly for the future scenarios along the full length of the estuary.

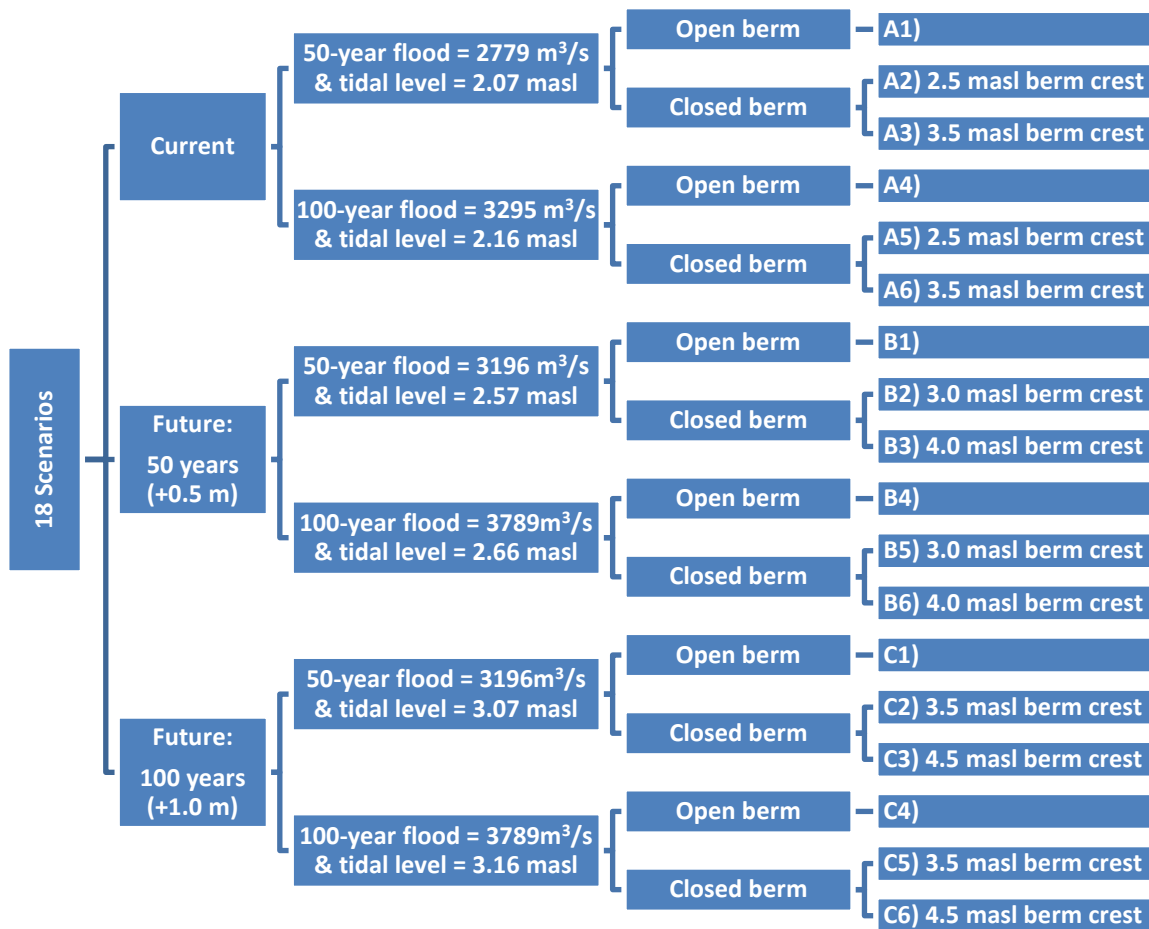


Figure 5. Hydrodynamic model scenarios

Simulated maximum flood levels along the estuary

From the output of the model simulations, the maximum water levels were obtained and the velocity head added to obtain the energy levels (to account for turbulent wave action). Figure 6 shows a long section of the simulated maximum water levels for scenario C. Note that the bed

levels are indicated for the current scenario and the berm crest is shown schematically only. The key findings from the simulation results are as follows: In the upper estuary the difference between the current and 100-year flood levels is approximately 0.9 m for Scenarios A and C. In the upper estuary the 100-year flood levels could rise by approximately 1.5 m, 100 years from now. In the lower estuary the difference between the 50- and 100-year flood levels with an initially closed berm is very small over approximately 6 km upstream of the mouth, for the current and future scenarios, and for both berm heights. In the lower estuary near the mouth the flood level can rise by approximately 1.2 m due to climate change and closed berm initial conditions, 100 years from now, for the highest berm scenario (similar to what could happen in the upper estuary). The initial crest level of an initial closed mouth condition plays an important role in the flood levels at the lower estuary. The berm breaches on the northern side near Witsand during the 50- and 100-year floods, while the southern berm remains generally intact after the flood. The simulated maximum flow velocities, as well as the breaching of the berm after a flood are shown in Figures 7 and 8, respectively.

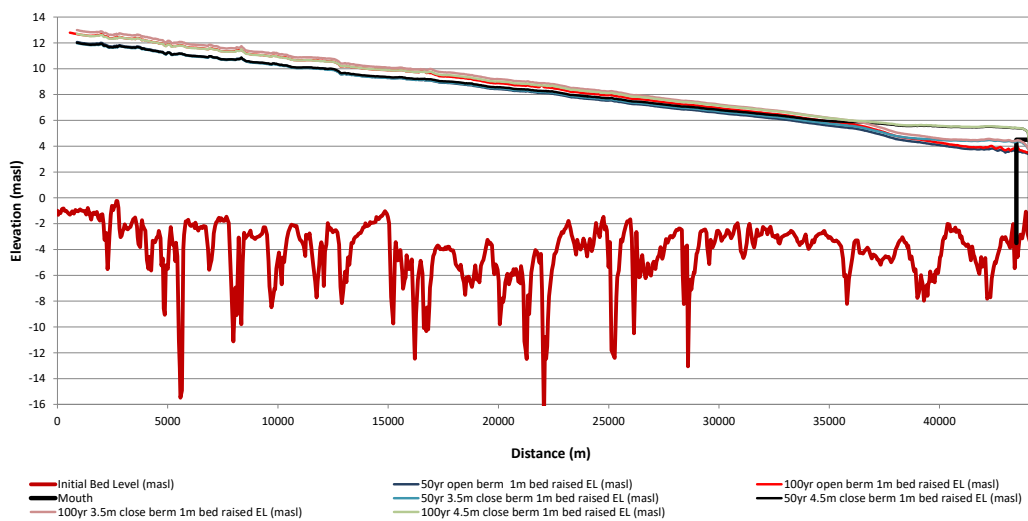


Figure 6. Simulated maximum routed flood levels along the estuary for the future Scenario C (100 years from now)

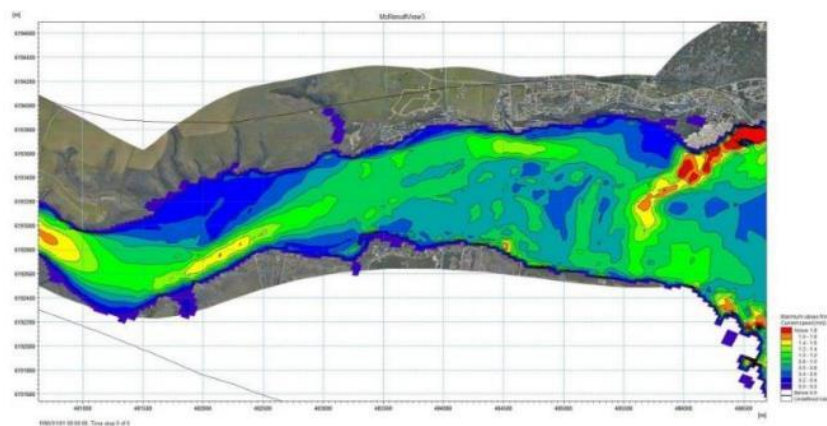


Figure 7. Simulated maximum flow velocities for current Scenario A1 in the lower estuary

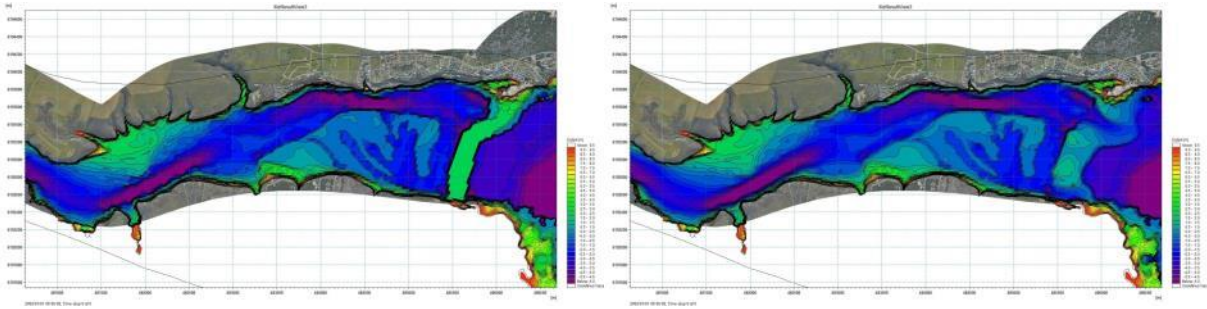


Figure 8. Simulated bed levels in the lower estuary for Scenario A5 before (left) and after (right) the flood

Simulation of Wave Heights

Background

Short waves originating from deep sea (swell) can penetrate an open estuary mouth and therefore can contribute to more extensive flood levels when its consequent wave runup is superimposed on a concurrent river flood level. For this purpose, the most critical swell direction causing maximum penetration into the lower estuary was found to be the East-southeasterly swell, which was transferred from deep sea through an open mouth into the estuary by means of the nearshore wave model, SWAN. The transfer of deep sea swell was simulated concurrently with a local wind blowing from the same sector over the entire SWAN model area. The resultant wave penetration into the estuary was therefore a combination of deep sea swell and locally wind generated waves. The 50- and 100-year wave and wind conditions were used to determine the spatial distribution of the penetrated wave conditions in the estuary and its consequent wave runup at eight locations in the lower estuary for the following flood line scenarios - (wave runup was derived with empirical methods with SWAN derived wave parameters and bank slopes):

- Scenario B1: 50-year ARI event, 50 years in the future with open estuary mouth
- Scenario B2: 50-year ARI event, 50 years in the future with closed initial estuary mouth
- Scenario C4: 100-year ARI event, 100 years in the future with open estuary mouth
- Scenario C6: 100-year ARI event, 100 years in the future with closed initial estuary mouth

Model setup and boundary conditions

The main input data required by SWAN included the bathymetry and estuary water levels as per the hydrodynamic model Mike21C for the different scenarios. A nesting approach was implemented whereby the waves were first computed on a coarse grid with a 500 m resolution, covering a larger seabed region (see Figure 9). The waves were then computed on a finer grid with a 50m resolution over the smaller region of interest (nested in the larger region) by employing the boundary conditions that were generated by the coarse grid computation. This approach was deemed necessary to ensure the mesh nearshore was sufficiently refined and to ensure the boundaries were distanced sufficiently far from the area of interest in the mouth.

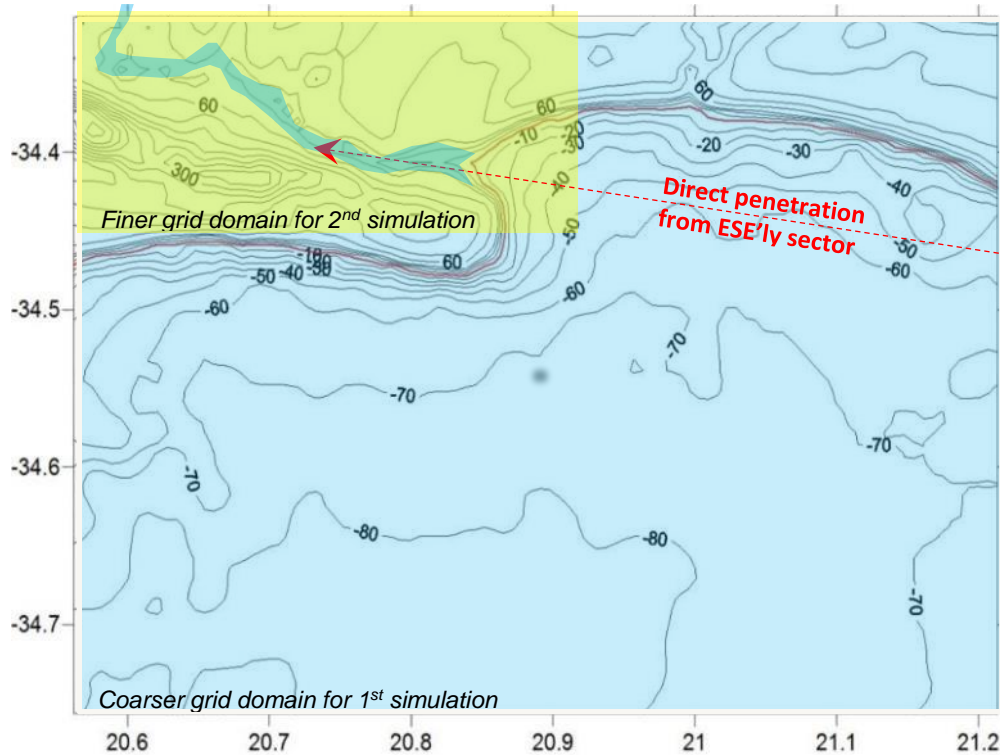


Figure 9. Seabed bathymetry from GEBCO data indicating the SWAN model domain

The following assumptions were made based on hindcast wave and wind data (ERA-Interim) from the ECMWF (European Centre for Medium-Range Weather Forecasts):

- The mouth was assumed to be completely washed open after the flood as shown in Figure 7. A Joint North Sea Wave Project (JONSWAP) spectrum with a peak enhancement factor (or wave spectrum gamma) of 1.75 and wave direction spreading of 30° specified the shape of the spectra at the computational grid boundaries.
- A significant deep sea swell wave height and mean wave period as per Table 6 with a wave direction of 110° specified the wave conditions at the wet boundaries of the coarse grid. This condition was identified as the critical swell condition for penetration into the estuary.
- Simulations were performed with a local wind blowing over the modelled area with a speed as per Table 6, with a nautical wind direction of 95°. This wind condition was initially identified as the critical locally generated condition which could be generated in the nearshore and penetrate into the estuary.

Table 6. Wind and wave conditions for the 50- and 100-year Annual Recurrence Interval (ARI) events

| Annual Recurrence Interval or ARI (years) | 50 | 100 |
|--|-----------------|------------------|
| Flood event | Q ₅₀ | Q ₁₀₀ |
| Extreme tidal levels (m) | 2.07 | 2.16 |
| Significant wave height (m)* | 5.9 | 6.2 |
| Mean wave period (sec)* | 11 | 12 |
| Wind speed (m/s)* | 19.1 | 20 |

*parameters assumed unaffected by climate change for the study area for future Scenarios B and C

Simulation results of lower estuary

The resulting significant wave heights and wave direction vectors, as well as the mean wave periods, for Scenario C4 are shown in Figures 10 and 11 respectively. Similar results with a maximum significant wave height of approximately 1.5 m were generated in the estuary for all scenarios. The critical point in the estuary is located on the left bank (north) at the Breede River Lodge where the largest wave heights and periods reach the estuary banks (Location 6 in Figure 12). The increased wave heights at the small bays (Locations 6, 7 and 8) are due to the wave shoaling effect at shallow river beds. The significant wave heights and peak wave periods yielded by the SWAN simulations are summarized for the four floodline scenarios and different locations in Table 7. Locations 2 and 4 have a flat slope and shallow slope with a large period while Locations 7 and 8 have a steep slope. Note the decreased wave heights at Locations 3 and 4 which imply that the wave effects are diminished further inward towards the river. Generally, Scenario B2 yields the largest wave heights.

Table 7. Significant wave heights and peak wave periods simulated by SWAN

| Scenario | Location | 1 | 2 | 3 | 4 | 5 | 6 | 7 | 8 |
|----------|----------|------|------|------|------|-------|-------|-------|-------|
| B1 | Hs (m) | 0.92 | 0.86 | 0.55 | 0.73 | 1.14 | 1.70 | 0.91 | 1.08 |
| | Tp (sec) | 8.80 | 5.87 | 2.84 | 7.44 | 9.10 | 11.12 | 7.53 | 9.47 |
| B2 | Hs (m) | 1.06 | 1.00 | 0.69 | 1.01 | 1.34 | 2.08 | 1.23 | 1.48 |
| | Tp (sec) | 7.76 | 5.72 | 3.69 | 7.13 | 8.75 | 11.66 | 9.08 | 11.03 |
| C4 | Hs (m) | 1.01 | 1.02 | 0.61 | 0.92 | 1.48 | 2.31 | 1.39 | 1.63 |
| | Tp (s) | 8.01 | 6.93 | 3.37 | 7.81 | 12.52 | 14.24 | 11.89 | 13.52 |
| C6 | Hs (m) | 0.58 | 0.79 | 0.66 | 0.91 | 1.24 | 1.92 | 0.95 | 1.22 |
| | Tp (s) | 4.01 | 3.98 | 2.96 | 5.26 | 7.89 | 11.88 | 6.36 | 9.09 |

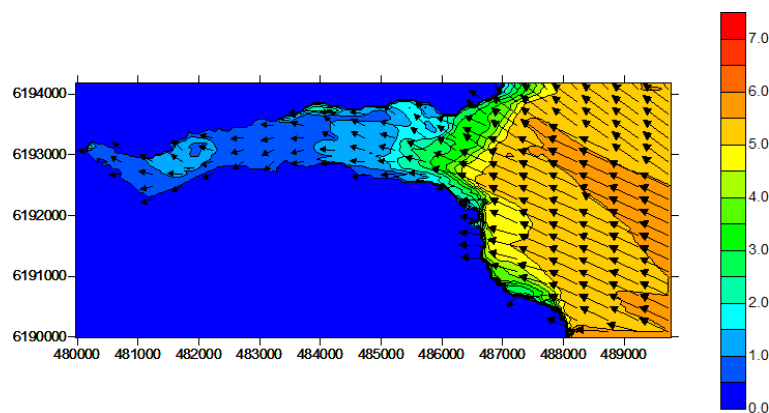


Figure 10. Contour map showing significant wave height with peak wave direction vectors for Scenario C4 (Hs in m)

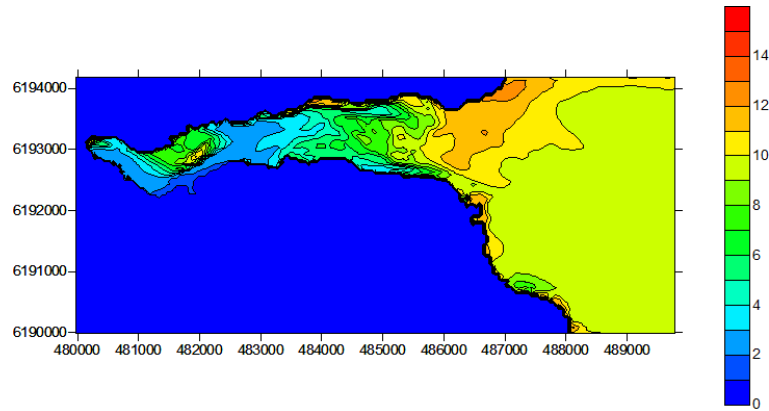


Figure 11. Contour map showing mean wave period for Scenario C4 (T_m in s)



Figure 12. Eight critical locations selected for wave runup calculations in the lower estuary

Runup Calculations

Wave runup is the extreme levels reached by oscillating waves on a slope, which is a function of wave height, wave period and bank slope, and could be more or less than the incident wave height. Wave runup for the wave height which is exceeded by 2% of the waves in the irregular wave train was derived with empirical methods at the eight critical locations. Three different empirical methods, namely EM as described in EurOtop II (2016), TAW (2002a), and Ahrens (1981), were considered to determine the wave runup for smooth slopes based on the significant wave height H_s and peak wave periods T_p simulated by SWAN. Refer to The Rock Manual (2007) (pages 487 to 517) for explanations of the methods used. The EM (2016) method is described in the EurOtop II Manual (2016) (pages 100 to 107) which states that this method may replace the other methods outlined in The Rock Manual. Therefore, for the purpose of this study the EM (2016) method took precedence over the other three methods. However, in cases where the EM (2016) method was not applicable, the average of the TWA (2002a) and Ahrens (1981) was used. The different methods produced very similar results. In addition, a reduction factor used to account for oblique wave attack at an approach angle. Table 8 gives the slope and reduction factors employed in the wave runup equations. Note that the significant wave heights yielded by SWAN account for the reduction in wave height caused by waves breaking on a shallow foreshore. Therefore, the equations for a shallow foreshore outlined in the EurOtop II Manual (2016) are not applicable.

Table 8. Slope and oblique wave attack parameters at different locations

| Location | 1 | 2 | 3 | 4 | 5 | 6 | 7 | 8 |
|--|----------|----------|----------|-----------------|----------|----------|----------|----------|
| Slope tan α (%) | 12.0 | 3.2 | 6.3 | 2.8 | 12.9 | 9.0 | 15.0 | 14.4 |
| Wave approach direction | 90° | 60° | 75° | 10° | 80° | 85° | 85° | 80° |
| Reduction factor | 0.82 | 0.87 | 0.84 | $\frac{0.9}{8}$ | 0.82 | 0.82 | 0.82 | 0.82 |

The runup heights for the different scenarios and locations are summarized in Table 9 and are defined as the vertical height above the concurrent flood level, i.e. the flood level obtained from the Mike21C model simulations. Scenario C4 experiences the highest wave runup of up to 4.12 m, particularly at Location 8, owing to its steepness. Despite this extreme value, the runup levels diminish from an average of 2 m at the river mouth to approximately 0.5 m inland. For the upper estuary, average runup heights of 0.75 m for the 100-year flood and 0.5 m for the 50-year flood were used.

Table 9. Wave runup heights above the concurrent flood levels for the selected floodline scenarios and locations (m)

| Location | 1 | 2 | 3 | 4 | 5 | 6 | 7 | 8 |
|--------------------|----------|----------|----------|----------|----------|----------|----------|----------|
| Scenario B1 | 1.66 | 0.30 | 0.22 | 0.35 | 2.05 | 2.14 | 1.76 | 2.33 |
| Scenario B2 | 1.57 | 0.32 | 0.32 | 0.39 | 2.14 | 2.48 | 2.47 | 3.17 |
| Scenario C4 | 1.58 | 0.39 | 0.27 | 0.41 | 3.22 | 3.20 | 3.50 | 4.12 |
| Scenario C6 | 0.60 | 0.20 | 0.25 | 0.27 | 1.85 | 2.43 | 1.52 | 2.37 |

Combined Flood Levels

Table 10 summarizes the Mike21C flood levels combined with the short wave runup results at the different locations in the lower estuary. The maximum water level at each location, between Scenarios B1 and B2, should be used to determine the proposed Breede River floodline for a 50-year flood. For future development, the 100-year flood is proposed, based on the maximum water levels at each location for Scenarios C4 and C6. Table 10 indicates the following: there is a relatively large range of maximum water levels depending how exposed the location is to waves; the initially closed mouth gives higher combined flood levels than the open mouth scenario; and Scenario B has higher water levels than some of the Scenario C values.

Table 10. Simulated combined river flood routed energy levels and wave runup at eight locations in the lower estuary (masl)

| Location: | 1 | 2 | 3 | 4 | 5 | 6 | 7 | 8 |
|----------------------|-------------|-------------|-------------|-------------|-------------|-------------|-------------|-------------|
| Scenario B1 | 4.38 | 3.38 | 3.66 | 3.90 | 5.31 | 5.35 | 4.86 | 5.36 |
| Scenario B2 | 5.76 | 4.79 | 4.87 | 4.96 | 6.63 | 6.93 | 6.93 | 7.60 |
| Maximum of B: | 5.76 | 4.79 | 4.87 | 4.96 | 6.63 | 6.93 | 6.93 | 7.60 |
| Scenario C4 | 4.90 | 4.26 | 4.51 | 4.73 | 7.20 | 7.10 | 7.46 | 8.12 |
| Scenario C6 | 5.84 | 5.71 | 5.79 | 5.79 | 7.35 | 7.90 | 7.06 | 7.87 |
| Maximum of C: | 5.84 | 5.71 | 5.79 | 5.79 | 7.35 | 7.90 | 7.46 | 8.12 |

For existing properties and infrastructure, the maximum 50-year floodline is proposed. The floor levels of existing dwellings should be above the floodline. For any new future infrastructure development or alterations/extensions to existing properties near the estuary, it is proposed that the maximum 100-year with climate change 100 years from now floodline is implemented.

Conclusions and Recommendations

The extreme flood levels in the Breede River Estuary were determined by modelling river floods and waves penetrating the estuary. A two dimensional hydrodynamic model was set up and calibrated against 1906 and 2008 historical flood levels and field data collected in 2017. Open and initially closed estuary mouth conditions were investigated with the movable bed model. Probabilistic hydrological methods were used to calculate the 50- and 100-year floods (i.e. 3196 and 3789 m³/s, respectively) which included a 15% increase for future climate change. The effect of climate change was further included in future scenarios 50 and 100 years from the present by raising the sea level 0.5 and 1.0 m, respectively. The initial estuary bed levels were also raised correspondingly for the future scenarios. However, the wind and wave conditions were assumed to remain unaffected by future climate change for the study site. The tidal boundary in the hydrodynamic model was set constant at the respective recurrence interval maximum tidal levels (based on observed data) and a long wave with a height of 0.7 m and a period of 180 s was also specified at the open boundary. The model simulated maximum water levels were increased with their respective velocity heads to obtain the energy levels, to account for turbulent flow wave action. In order to finally determine the floodlines for the Breede River Estuary, the short wave runup heights on the estuary banks were also determined and then added to the routed energy levels. Short waves originating from deep sea (swell) can penetrate an open estuary mouth and therefore can contribute to more extensive flood levels when its consequent wave runup is superimposed on a concurrent river flood level. For this purpose, the most critical swell direction causing maximum penetration into the lower estuary (i.e. swell from the east-southeasterly direction) was considered. The transfer of the east-southeasterly swell from deep sea into the estuary was done concurrently with a local wind blowing from the same sector over the entire SWAN model area. The resultant wave penetration into the estuary was therefore a combination of deep sea swell and locally wind generated waves. It was found that the swell and wind conditions for the 50- and 100-year recurrence intervals do not differ significantly. The 50- and 100-year wave and wind conditions were used to determine the spatial distribution of the penetrated wave conditions in the estuary and its consequent wave runup at eight locations in the lower estuary. The highest flood line level (flood energy level plus wave runup) of 8.1 masl was calculated near the mouth for the future climate change scenario, 100 years from the present.

For existing residential and other properties and infrastructure the maximum floodline levels of Scenarios B1 and B2 in Table 10 are proposed. The scenarios are based on the 50-year flood with 50-year future climate change considered, as well as an open mouth or a low closed mouth berm crest level as initial condition in order to obtain conservatively high flood levels in the lower Breede River estuary. For any new future infrastructure or development near the estuary, the maximum floodline levels of Scenarios C4 and C6 in Table 10 is implemented are proposed.

Acknowledgements

The authors wish to thank the Western Cape Government Department of Environmental Affairs and Development planning (WC DEA&DP) for their permission to publish this paper. The opinions and views presented in this paper are, however, those of the authors and do not necessarily reflect those of the WC DEA&DP.

References

- CIRIA, CUR, CETMEF (2013) .The Rock Manual. The use of rock in hydraulic engineering, 2nd Edition. Delft University of Technology.
- ECMWF Data centre. <http://www.ecmwf.int/en/research/climate-reanalysis/browse-reanalysis-datasets>.
- EurOtop (2016). Manual on wave overtopping of sea defences and related structures. An overtopping manual largely based on European research, but for worldwide application. Van der Meer, J.W., Allsop, N.W.H., Bruce, T., De Rouck, J., Kortenhaus, A., Pullen, T., Schüttrumpf, H., Troch, P. and Zanuttigh, B., www.overtopping-manual.com
- GEBCO 30 arc-second global grid of elevations, GEBCO_2014 Grid (2014). http://www.gebco.net/data_and_products/gridded_bathymetry_data/gebco_30_second_grid/
- IPCC Intergovernmental Panel on Climate Change (2013). The Physical Science Basis. Working Group I. Contribution to the Fifth Assessment Report of the Intergovernmental Panel on Climate Change. <http://ipcc.ch/report/ar5/>
- Mentaschi, L., M. I. Vousdoukas, E. Voukouvalas, A. Dosio, and L. Feyen (2017). Global changes of extreme coastal wave energy fluxes triggered by intensified teleconnection patterns, University of Hawaii, Seal Level Centre (UHSLC). Recorded tidal data at <http://uhslc.soest.hawaii.edu/>
- Wang L W et al (2014). Changes in global ocean wave heights as projected using multi-model CMIP5 simulations. Climate Research Division, Science and Technology Branch, Environment Canada, Toronto, Ontario, Canada.